

## Genetic Landscapes of Relapsed and Refractory Diffuse Large B-Cell Lymphomas

Ryan D. Morin<sup>1,2</sup>, Sarit Assouline<sup>3,4</sup>, Miguel Alcaide<sup>1</sup>, Arezoo Mohajeri<sup>1</sup>, Rebecca L. Johnston<sup>5</sup>, Lauren Chong<sup>5</sup>, Jasleen Grewal<sup>1</sup>, Stephen Yu<sup>1</sup>, Daniel Fornika<sup>1</sup>, Kevin Bushell<sup>1</sup>, Torsten Holm Nielsen<sup>6</sup>, Tina Petrogiannis-Haliotis<sup>7</sup>, Michael Crump<sup>8</sup>, Axel Tosikyan<sup>9</sup>, Bruno M. Grande<sup>1</sup>, David MacDonald<sup>10</sup>, Caroline Rousseau<sup>11</sup>, Maryam Bayat<sup>4</sup>, Pierre Sesques<sup>3</sup>, Remi Froment<sup>3</sup>, Marco Albuquerque<sup>1</sup>, Yury Monczak<sup>7</sup>, Kathleen Klein Oros<sup>12</sup>, Celia Greenwood<sup>12,13,14</sup>, Yasser Riazalhosseini<sup>15</sup>, Madeleine Arseneault<sup>15</sup>, Errol Camlioglu<sup>16</sup>, André Constantin<sup>16</sup>, Qiang Pan-Hammarstrom<sup>17,18</sup>, Roujun Peng<sup>17,18</sup>, Koren K. Mann<sup>3,4</sup>, and Nathalie A. Johnson<sup>3,4</sup>

### Abstract

**Purpose:** Relapsed or refractory diffuse large B-cell lymphoma (rrDLBCL) is fatal in 90% of patients, and yet little is known about its biology.

**Experimental Design:** Using exome sequencing, we characterized the mutation profiles of 38 rrDLBCL biopsies obtained at the time of progression after immunochemotherapy. To identify genes that may be associated with relapse, we compared the mutation frequency in samples obtained at relapse to an unrelated cohort of 138 diagnostic DLBCLs and separately amplified specific mutations in their matched diagnostic samples to identify clonal expansions.

**Results:** On the basis of a higher frequency at relapse and evidence for clonal selection, *TP53*, *FOXO1*, *MLL3* (*KMT2C*), *CCND3*, *NFKB1Z*, and *STAT6* emerged as top candidate genes implicated in therapeutic resistance. We observed individual

examples of clonal expansions affecting genes whose mutations had not been previously associated with DLBCL including two regulators of NF- $\kappa$ B: *NFKB1E* and *NFKB1Z*. We detected mutations that may affect sensitivity to novel therapeutics, such as *MYD88* and *CD79B* mutations, in 31% and 23% of patients with activated B-cell-type of rrDLBCL, respectively. We also identified recurrent *STAT6* mutations affecting D419 in 36% of patients with the germinal center B (GCB) cell rrDLBCL. These were associated with activated JAK/STAT signaling, increased phospho-STAT6 protein expression and increased expression of *STAT6* target genes.

**Conclusions:** This work improves our understanding of therapeutic resistance in rrDLBCL and has identified novel therapeutic opportunities especially for the high-risk patients with GCB-type rrDLBCL. *Clin Cancer Res*; 22(9); 2290–300. ©2015 AACR.

### Introduction

Diffuse large B-cell lymphoma (DLBCL) is the most common non-Hodgkin lymphoma (NHL) and is curable in approximately 60% of patients with multi-agent chemotherapy, such as rituximab, cyclophosphamide, doxorubicin, vincristine, and prednisone (R-CHOP; ref. 1). DLBCL can be classified into two cell-of-origin (COO) molecular subtypes, the germinal center

B-cell (GCB) type and activated B-cell (ABC) type, where the latter is associated with an inferior outcome (2, 3). DLBCL can also evolve from histologic transformation of a pre-existing indolent lymphoma (Tly), most commonly follicular lymphoma. Patients with relapsed or refractory Tly (rrTly) and DLBCL (rrDLBCL) have a poor outcome, with only approximately 40% of patients achieving long-term remissions with salvage chemotherapy and autologous stem cell transplant (SCT; ref. 4).

<sup>1</sup>Department of Molecular Biology and Biochemistry, Simon Fraser University, Burnaby, British Columbia, Canada. <sup>2</sup>Genome Sciences Centre, BC Cancer Agency, Vancouver, British Columbia, Canada. <sup>3</sup>Department of Medicine, Jewish General Hospital, Montreal, Quebec, Canada. <sup>4</sup>McGill University, Montreal, Quebec, Canada. <sup>5</sup>University of British Columbia, Vancouver, British Columbia, Canada. <sup>6</sup>Department of Internal Medicine, Copenhagen University Hospital, Roskilde, Denmark. <sup>7</sup>Department of Pathology, Jewish General Hospital, Montreal, Quebec, Canada. <sup>8</sup>Princess Margaret Hospital, Toronto, Ontario, Canada. <sup>9</sup>Sacre-Coeur Hospital, Montreal, Quebec, Canada. <sup>10</sup>Department of Medicine, University of Dalhousie, Halifax, Nova Scotia, Canada. <sup>11</sup>Quebec Clinical Research Organization in Cancer, Montreal, Quebec, Canada. <sup>12</sup>Lady Davis Institute, Jewish General Hospital, Montreal, Quebec, Canada. <sup>13</sup>Department of Epidemiology, Biostatistics and Occupational Health, McGill University, Montreal, Quebec, Canada. <sup>14</sup>Department of Oncology, McGill University, Montreal, Quebec, Canada. <sup>15</sup>Department of Human Genetics, McGill University, Montreal, Quebec, Canada. <sup>16</sup>Department of Radiology, Jewish General Hospital, Montreal, McGill University, Quebec,

Canada. <sup>17</sup>Clinical Immunology, Department of Laboratory Medicine, Karolinska Institute at Karolinska University Hospital, Huddinge, Sweden. <sup>18</sup>Department of Medical Oncology, Sun Yat-sen University Cancer Center, State Key Laboratory of Oncology in South China.

**Note:** Supplementary data for this article are available at Clinical Cancer Research Online (<http://clincancerres.aacrjournals.org/>).

R.D. Morin, S. Assouline, K.K. Mann, and N.A. Johnson contributed equally to this article.

**Corresponding Author:** Nathalie A. Johnson, Departments of Medicine and Oncology, Jewish General Hospital, Room E-725, 3755, chemin de la Cote-Ste-Catherine, Montreal, Quebec H3T 1E2, Canada. Phone: 514-340-8707; Fax: 514-340-8733; E-mail: [nathalie.johnson@mcgill.ca](mailto:nathalie.johnson@mcgill.ca)

doi: 10.1158/1078-0432.CCR-15-2123

©2015 American Association for Cancer Research.

### Translational Relevance

Despite an improved understanding of the biology of *de novo* diffuse large B-cell lymphoma (DLBCL), the outcome of patients with relapsed and refractory (rrDLBCL) is still poor. Response rates to novel therapies that target specific pathways may depend on the tumor's mutation profile, which is unknown for patients with rrDLBCL at the time of relapse. We identified genes that are recurrently mutated at a higher frequency at relapse compared with diagnosis. We also provide evidence for clonal expansion of some mutations using paired diagnostic-relapse samples taken from the same patients. These mutations should be studied further as potential biomarkers of resistance to RCHOP chemotherapy. Our results highlight that JAK/STAT and NF- $\kappa$ B pathways are commonly altered in rrDLBCL, nominating these as promising avenues for targeted therapeutics. Although NF- $\kappa$ B has been heavily pursued as a target in DLBCL, the relevance of the JAK/STAT pathway in rrDLBCL has not been appreciated.

The genetic landscape of *de novo* DLBCL is well characterized. Genomic alterations contribute to escape from immune surveillance, inhibit DNA damage response and apoptosis, promote survival pathways, or reprogram the epigenetic landscape of the tumor (5–16). Although DLBCL shares some commonalities across COO types, the mutation frequency of some genes is enriched only in one subtype. Genomic analysis of paired follicular lymphoma and Tly samples revealed that Tly is genetically more complex than follicular lymphoma and has genetic features associated with both GCB-DLBCL and ABC-DLBCL (17, 18). However, most Tly samples analyzed to date were collected after chemotherapy, making it challenging to differentiate whether genetic changes distinguishing *de novo* GCB-DLBCL from Tly contribute to histologic transformation or result from clonal selection induced by chemotherapy (17, 18).

Subsequent to a selective pressure, such as R-CHOP treatment, chemotherapy-resistant subclones that survive may be enriched at the time of relapse due to clonal expansions. Obtaining a biopsy at the time of progression provides an opportunity to identify genomic alterations unique to these populations of cells. However, rrDLBCL samples are rare because patients are not routinely rebiopsied at the time of relapse outside the context of a clinical trial. Given that very few patients survive rrDLBCL, there is also a lack of constitutional DNA for most archived samples, which is important to exclude germline variants when performing whole-exome sequencing (WES). For such reasons, the genomic profile of rrDLBCL is not well known, with two small cohorts of approximately 10 patients described in the literature to date (19, 20). Characterizing a sufficient number of rrDLBCL samples may lead to insights into the genetic events that lead to therapeutic resistance and reveal pathways that are consistently activated at relapse, some of which may be targeted with existing or novel therapies.

Herein, we report the mutational landscape of 38 samples of rrDLBCL and rTly, determined using WES. Many genes mutated in this cohort have been reported with variable frequencies in diagnostic DLBCL, Tly, primary mediastinal B-cell lymphoma

(PMBCL), and follicular lymphoma (5, 7–10, 17, 18, 21, 22). On the basis of comparison with published data on *de novo* DLBCL and evidence for clonal expansion in paired biopsies, we find a higher prevalence of mutations affecting six genes at relapse, including the transcription factor *STAT6*. The recurrent mutation we observe affecting the D419 residue has been reported to activate JAK/STAT signaling in follicular lymphoma and conferred sensitivity to JAK2 inhibitors in PMBCL (22, 23). We show that *STAT6* D419 mutations may similarly activate JAK/STAT signaling in the GCB-rrDLBCL and rTly (22). With the exception of PMBCLs, this pathway has not previously been implicated in *de novo* DLBCL.

## Materials and Methods

### Sample acquisition

This study included three DLBCL cohorts stratified based on the timing of sample acquisition. The first "relapse" cohort consisted of 38 patients whose samples were obtained after at least one cycle of immunochemotherapy, of which 25 evolved from *de novo* DLBCL, and 13 were Tly. Cases were selected on the basis of availability of both tumor tissue and germline DNA. In 27 of 38 cases, samples were obtained prospectively from patients enrolled on the Quebec Clinical Research Organization in Cancer (QCROC-2) clinical trial NCT01238692 (QC2- identifiers). In the remaining 11 of 38, eight were analyzed in the context of another study focusing on DLBCL in the Chinese population (CH-identifiers; ref. 20), and three samples were from patients treated in Montreal, Quebec (MT- samples). In 12 of 38 patients, we had matched pairs, where one sample was taken at diagnosis before RCHOP and a second tumor sample was taken at relapse. The clinical details and the type of analysis performed on each sample are provided in Supplementary Table S1. The second "diagnostic" cohort consisted of a different set of 138 patients with *de novo* DLBCL, for which good quality WES or genome data was publically available for reanalysis (7–10). This was used as the "control" group representing diagnostic DLBCL. The third "pretreatment" cohort consisted of 49 patients selected on the basis of the availability of tissue of their diagnostic DLBCL ( $n = 27$ ) or Tly ( $n = 22$ ) taken prior to initiation of therapy. These cases were used as pretreatment "controls" for the targeted resequencing of *STAT6* and other genes of interest (Supplementary Table S2). The diagnosis of DLBCL was confirmed by histopathology review, using the 2008 World Health Organization criteria (24). All patients provided informed consent either for the clinical trial or for storage of samples in a databank. This project was approved by the research ethics boards at the Jewish General Hospital and is in accordance with the declaration of Helsinki.

### Sample preparation for the QCROC-2 trial

Four core-needle biopsies were performed for the 27 patients with rrDLBCL enrolled on the clinical trial. One core was fixed in formalin and embedded in paraffin (FFPET) for protein detection by immunohistochemistry (IHC). The remaining three cores were pooled in RPMI medium and DLBCL cells were enriched using a magnetic bead–negative selection technique (human B-cell enrichment cocktail without CD43; Stem Cell technologies) as previously described (25). DNA and RNA from purified B cells and peripheral blood mononuclear cells were isolated using the AllPrep kit (Qiagen).

### Immunohistochemical analysis

For 25 of 27 of the clinical trial patients, slides containing 5  $\mu\text{m}$  of FFPET were used to determine the protein expression of phospho-STAT6 (rabbit polyclonal anti-Tyr641; Cell Signaling Technology) using an automated Ventana system (Roche) and >10% of cells was considered positive using previously published thresholds (23). Tumor content was estimated by the number of tumor cells by hematoxylin and eosin stain and CD20 expression (clone L26; Dako) in the QCROC-2 cases prior to B-cell enrichment (Supplementary Table S1). Because of the low quantity of cells obtained after B-cell selection, tumor content was not reassessed. In patients where gene expression profiling was not available or called "unclassifiable," COO assignment was determined on the basis of Hans criteria (26).

### Exome sequencing and analysis

Tumor and germline samples were sequenced using exome capture in 38 patients with 100 nt paired reads using the HiSeq 2000 platform (Illumina). Somatic variants were detected using Strelka with the depth filter disabled (27). We implemented a custom filter to discount variant base calls deriving from the same fragment to mitigate an increased rate of false variant calls observed in libraries with a significant number of overlapping reads. Known single-nucleotide polymorphisms were not filtered from the analysis because all tumors were analyzed with matched normal DNA. Exome data were separately analyzed for somatic copy number variation (CNV) and loss of heterozygosity (LOH) using TITAN (28).

To facilitate comparison of mutation prevalence between relapsed DLBCL and diagnostic tumors, we obtained the raw sequence data from 138 diagnostic DLBCL tumor/normal pairs from four published studies and reanalyzed these for single-nucleotide variants (SNV) and insertions or deletions (indels) using a similar approach (7–10, 20).

### Targeted sequencing of candidate genes

We performed targeted sequencing in 30 of 38 rrDLBCL samples to determine the variant allele fraction (VAF) of genes that were frequently mutated in the exomes and/or had a role in diagnostic DLBCL (provided in Supplementary Methods). *FOXO1* was included because it is known to be associated with a poor outcome in DLBCL and had poor coverage across most exomes (29). In 12 patients, we performed deep sequencing of selected mutations in paired DLBCL biopsies (diagnosis/relapse) taken from the same patients. Targeted sequencing of *STAT6* and other genes was also performed in the "pretreatment" cohort of 49 patients to determine the frequency of these mutations obtained using a deep-sequencing approach in diagnostic DLBCL and Tly samples obtained prior to chemotherapy.

### Gene expression profiling and gene-set enrichment analysis

We isolated RNA from purified lymphoma cells that was used in cDNA microarray analyses using either the Sureprint 8  $\times$  60K one-color human expression array (Agilent) or the Human Gene 2.0 ST array (Affymetrix) platforms. We calculated the COO (LLMP score) using the subgroup of predictor genes identified by Wright and colleagues (30). Refer to Supplementary Methods for the methodology of normalization of platforms and the gene expression analysis of *STAT6*-mutant rrDLBCL.

## Results

### The mutational spectrum of relapsed or refractory DLBCL and Tly

The mutational profiles of the 38 rrDLBCL and Tly samples illustrated in Fig. 1 demonstrates that genetic heterogeneity is a hallmark of this disease, even following treatment. The complete exome and targeted sequencing data are found in Supplementary Tables S3 and S4, respectively. The average mutation load was higher in the trial samples relative to the archival rrDLBCLs (119.1 and 63.7 non silent SNVs, respectively;  $P = 0.032$ ), but the most common mutations were evenly distributed between both groups, which were combined for subsequent analyses. We also identified somatic copy number alterations (CNA) using the WES data and observed many events known to be common in *de novo* DLBCL (Supplementary Fig. S1).

The genes commonly mutated at relapse and additional ones known to contribute to the pathogenesis of *de novo* DLBCL were ranked in decreasing order of frequency in Table 1. The genes most commonly mutated in ABC rrDLBCL were *PIM1* (38%), *MYD88* (31%), *MLL3* (23%), and *CD79B* (23%). The most common GCB rrDLBCL-enriched mutations were *CREBBP* (45%), *STAT6* (36%), and *FOXO1* (36%) followed by *BCL2* and *EZH2* in 27% of samples. The most common mutations that were not COO-specific were *TP53* (32%), *MLL2* (*KMT2D*) (28%) and *FAS* (16%). Given their known roles as tumor suppressor genes, *FAS*, *MLL2*, *TP53*, and *CREBBP* bore a general pattern of inactivating mutations. In contrast, *MYD88* (L265), *EZH2* (Y641), *FOXO1*, and *STAT6* were genes in which mutations recurred at hot spots, indicating they were likely functionally significant (6, 15, 21, 29).

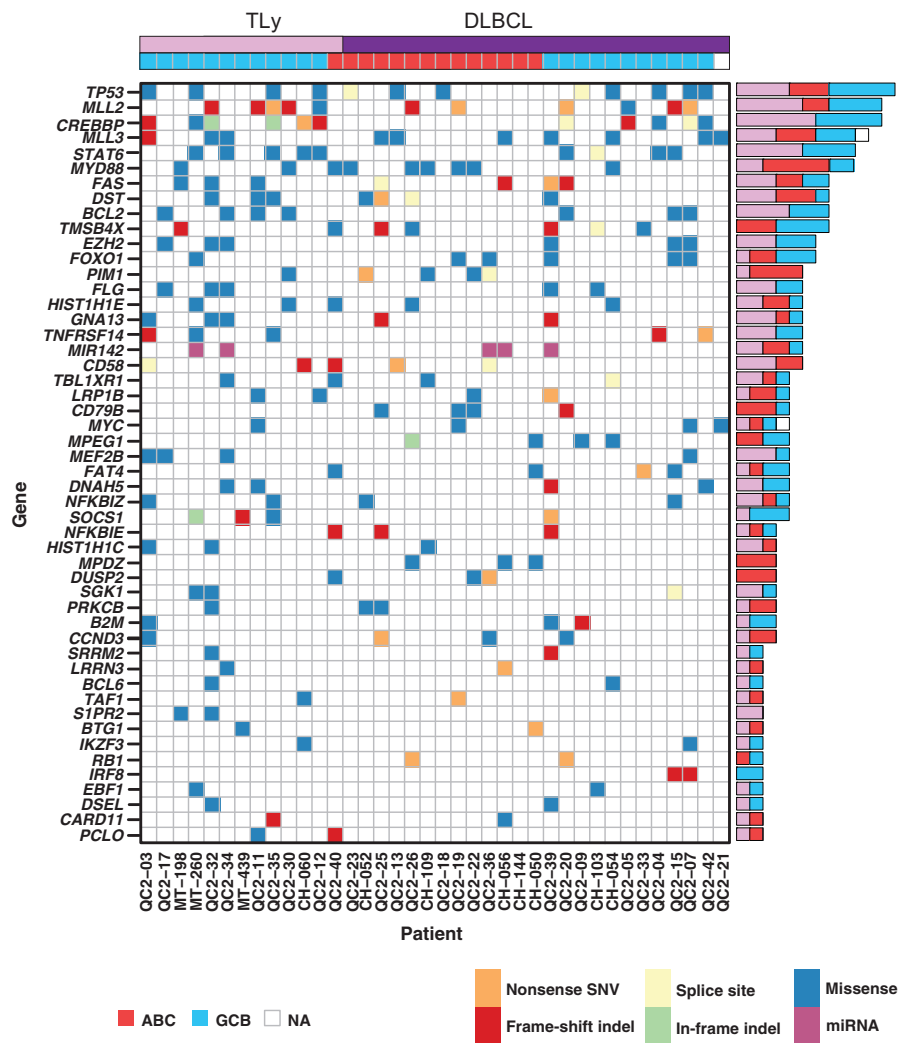
The mutation profile of rrTly was very similar to GCB-rrDLBCL. Tly represented mainly transformed follicular lymphoma (11/13 cases), all of which had a GCB phenotype. One case arose from a marginal zone lymphoma and classified as GCB. The last case arose from Waldenstrom macroglobulinemia, which harbored a *MYD88* mutation and was classified as ABC. Mutations in *STAT6* and *FAS*, two genes that were previously reported to be a consequence of histologic transformation of follicular lymphoma, were equally distributed in GCB-type rrDLBCL and rrTly (17, 18). In contrast, there was a higher frequency of *FOXO1* mutations in GCB-rrDLBCL relative to rrTly cases. Thus, even in the relapse setting, the genetic profile of ABC-rrDLBCL is different from GCB-rrDLBCL and rrTly.

### Clonal selection for driver mutations

To search for genes with a potential role in therapeutic resistance, we used two complementary approaches. First, we compared the mutation frequency obtained by WES in the "relapse" rrDLBCL cohort ( $n = 25$ ) to a separate "diagnostic" DLBCL cohort ( $n = 138$ ) and excluded the 13 cases of rrTly for this analysis. On the basis of this comparison, seven genes were significantly more commonly mutated among the "relapse" samples, namely: *MLL3*, *MPEG1*, *NFKBIZ*, *CCND3*, *STAT6*, *TP53*, and *MYC* ( $P < 0.05$ ; Table 1). The mutations in *MYC* and *CCND3* affected hot spots previously reported in Burkitt lymphoma, where mutations have been shown to increase protein stability, such as I290R and Q276X in *CCND3* and T73A and P74A in *MYC* (31, 32). Because of systematic low coverage of *FOXO1* among exomes (Supplementary Figs. S2 and S3), we separately compared the prevalence of *FOXO1* mutations in our rrDLBCLs to a large published cohort of 279 untreated DLBCLs (29). This revealed a significant

**Figure 1.**

Overview of somatic mutations identified in 38 rrDLBCLs and rrTly. Mutations affecting genes previously identified as significant mutation targets in DLBCL and any additional genes found mutated in our cohort in at least three samples are shown. Each column corresponds to a sample where the patient identifiers are below and cases are ordered by the lymphoma type with rrTly on the left (pink bar) and rrDLBCL on the right (purple bar). Cell of origin (COO) is indicated to designate GCB cases in blue and ABC cases in red. One case could not be assigned a COO and is shown in white. The type of coding mutation is indicated in the figure legend. Noncoding mutations are omitted with the exception of mutations affecting the miRNA gene MIR142 (purple), which were observed in multiple cases of rrDLBCL and rrTly.



enrichment of *FOXO1* mutations among rrDLBCLs (8.6% vs. 27%,  $P = 0.022$ ; ref. 29), thereby nominating this as an eighth gene for which mutations may be more common at relapse.

We then analyzed 12 tumor pairs derived from the same patients, where one sample was obtained at diagnosis and one at relapse and determined whether mutations found at relapse were acquired or resulted from expansion of subclones present at diagnosis. We calculated the VAF for selected mutations, which is proportional to the fraction of cells in the tumor carrying a given mutation, but can also be affected by tumor purity and CNV. Figure 2 illustrates that there are variations in VAF for different mutations at diagnosis and at relapse, suggesting that clonal evolution can occur following RCHOP therapy. We found evidence for clonal expansions of at least one mutation in 11 of 12 paired-samples affecting mutations in 23 genes (Table 2; Supplementary Fig. S4). Some mutations were present, but subclonal at diagnosis, and subsequently appeared in a larger fraction of cancer cells at relapse. This was observed for some of the mutations in *BCL2*, as well as mutations affecting *RB1*, *EZH2*, *MYD88*, *NFKBIE*, *FOXO1*, *TNFRSF14*, *CARD11*, *B2M*, and *STAT6*. We also found examples of mutations that were detectable and often clonal at relapse, but were undetectable in the diagnostic specimen. This

was the case for additional *BCL2*, *STAT6*, *FOXO1*, and *TNFRSF14* mutations along with those affecting *TP53*, *CD79B*, *NFKBIZ*, *SOCS1*, *MLL3*, *MEF2B*, *ARID1A*, *CCND3*, *MLL2*, and *TBL1XR1*. Taken together, our data support that clonal expansion of some mutations can occur following RCHOP. Importantly, many of the mutations present in the dominant clone at relapse could not be detected by deep sequencing the diagnostic biopsies of these same patients, indicating that these either existed in an exceedingly small subpopulation of cells, a separate population of cells not sampled by the biopsy, or that they were acquired *de novo* in the intervening time between diagnosis and relapse. Overall, we found multiple examples of tumors exhibiting clonal expansion of *STAT6* mutations (3 cases) or other genes in this pathway (e.g., *SOCS1*, 2 cases), as well as those affecting *FOXO1* (3 cases), *NFKBIE* (2 cases), *MLL2* (2 cases), and *CD79B* (2 cases).

On the basis of prevalence at relapse and examples of clonal expansions, mutations in multiple genes emerged as potential candidates for contributing to therapeutic resistance in DLBCL. By considering enrichment in our rrDLBCL cohort in conjunction with clonal selection, we became particularly interested in *TP53*, *FOXO1*, *MLL3*, *CCND3*, *NFKBIZ*, and *STAT6*. Notably, in some cases, there was also evidence of copy number variation at relapse

**Table 1.** Frequency of mutations in relapsed or refractory DLBCL and TLy

Gene mutated	% Mutations rrDLBCL N = 25 <sup>c</sup>	% Mutations ABC N = 13	% Mutations GCB N = 11	% Mutations TLy N = 13	% Mutations Dx DLBCL N = 138
<i>TP53</i> <sup>a</sup>	32	23	45	31	13
<i>MLL2</i>	28	15	36	38	13
<i>MLL3</i> <sup>a</sup>	28	23	27	23	7
<i>FOXO1</i> <sup>a,b</sup>	24	15	36	8	9
<i>CREBBP</i>	20	0	45	46	13
<i>MYD88</i>	20	31	9	23	12
<i>PIM1</i>	20	38	0	8	14
<i>STAT6</i> <sup>a</sup>	16	0	36	38	4
<i>FAS</i>	16	15	18	23	7
<i>CD79B</i>	16	23	9	0	9
<i>MPEG1</i> <sup>a</sup>	16	15	18	8	3
<i>BCL2</i>	12	0	27	31	10
<i>EZH2</i>	12	0	27	23	13
<i>CCND3</i> <sup>a</sup>	12	15	9	8	1
<i>MYC</i> <sup>a</sup>	12	8	9	8	2
<i>GNA13</i>	8	8	9	23	14
<i>CD58</i>	8	15	0	23	7
<i>NFKBIE</i>	8	8	9	8	1
<i>B2M</i>	8	0	18	8	12
<i>NFKBIZ</i> <sup>a</sup>	8	8	9	15	0
<i>TNFRSF14</i>	8	0	18	23	8
<i>MEF2B</i>	4	0	9	23	8
<i>SOCS1</i>	4	0	9	15	1
<i>CARD11</i>	4	8	0	8	12

NOTE: These genes were selected and ranked based on their overall frequency by exome sequencing in rrDLBCL that excluded cases of TLy.

Abbreviations: Dx, diagnosis; TLy, a DLBCL arising in the context of histologic transformation from an indolent lymphoma.

<sup>a</sup>Genes indicated in the table above are significant at a threshold of  $P < 0.05$ . Raw P values are as follows: *MPEG1*:  $P = 0.020$ ; *MLL3*:  $P = 0.020$ ; *CCND3*:  $P = 0.026$ ; *STAT6*:  $P = 0.033$ ; *TP53*:  $P = 0.033$ ; *NFKBIZ*:  $P = 0.023$ ; and *MYC*:  $P = 0.047$ .

<sup>b</sup>The frequency of *FOXO1* mutations is based on targeted sequencing of 18 QC2-rrDLBCL samples and the frequency in 279 diagnostic samples based on the study by Trinh and colleagues (29).

<sup>c</sup>In one rrDLBCL sample, the molecular subtype was not available, thus it was not included in the GCB or ABC categories. That case harbored mutations in *MLL2*, *MLL3*, and *MYC*.

but our methodology was not capable of ascertaining whether each CNV was present in the diagnostic specimen (Supplementary Fig. S5).

#### Novel mutations affecting NF- $\kappa$ B in rrDLBCL

Multiple genes with roles in NF- $\kappa$ B signaling showed either increased mutation prevalence in our cohort and/or evidence for clonal enrichment at relapse including *CARD11*, *CD79B*, *MYD88*, *NFKBIE*, and *NFKBIZ*. The latter two genes were mutated in 7/38 (18%) of rrDLBCLs representing both GCB and ABC cases. Despite the known role of NF- $\kappa$ B in ABC-type *de novo* DLBCLs, neither gene has previously been associated with *de novo* DLBCL. *NFKBIE* encodes I $\kappa$ B $\epsilon$ , which inhibits NF- $\kappa$ B-mediated transcription (33). Loss of I $\kappa$ B $\epsilon$  is known to increase B-cell proliferation via autocrine IL6 signaling (34) and inactivating mutations in *NFKBIE* have been reported in Hodgkin lymphoma (HL) and chronic lymphocytic leukemia (CLL; refs. 35–37). All three *NFKBIE*-mutated rrDLBCLs in our cohort carried the same frameshift indel, suggesting a strong selection for this variant to inactivate this gene (Supplementary Fig. S6). This is the same 4-nt deletion mutation that has recently been reported in aggressive cases of CLL (37). We sequenced *NFKBIE* in 27 additional cases of untreated DLBCLs and detected two additional examples of this indel and two other missense SNVs (Supplementary Table S5). *NFKBIZ* encodes I $\kappa$ B $\zeta$ , which regulates a set of NF- $\kappa$ B target genes that have been shown to promote the survival of ABC-DLBCL (38). The pattern of mutations affecting *NFKBIZ* were not clearly inactivating, com-

prising missense mutations largely restricted to the Ankyrin repeats. Taken together, the observation of mutations in genes involved in regulating NF- $\kappa$ B, including two genes with no previously established role in DLBCL, warrants further exploration on the role of these genes in the context of relapse.

#### Selection for mutant *STAT6* D419 in post-treatment TLy and GCB-DLBCL

We further examined the potential role of *STAT6* given its novelty in the context of *de novo* DLBCL and its reported role in JAK/STAT signaling, thereby nominating it as a potential therapeutic target. Of the nine *STAT6* mutations detected in our relapse cohort, all but one affected a single amino acid (D419) in the highly conserved site within the DNA-binding domain. D419 is a reported polymorphism in online databases, but in our series, we confirmed that these were somatic mutations because the variant allele was not present or  $< 1\%$  in the germline. D419 mutations were restricted to GCB-rrDLBCL (36%) and rrTLy (38%), and were absent in ABC rrDLBCL (0%), further supporting that these were not polymorphisms but rather mutations associated with a specific tumor biology (Table 1). Because our analysis of paired biopsies indicated that *STAT6* mutations may exist subclonally (e.g., as low as 1%) in diagnostic samples, we performed deep sequencing of *STAT6* in an extended "pretreatment" cohort, consisting of *de novo* DLBCL and TLy samples taken prior to chemotherapy, to determine the incidence of clonal and subclonal *STAT6* mutations in diagnostic tumors. We observed coding mutations in 4

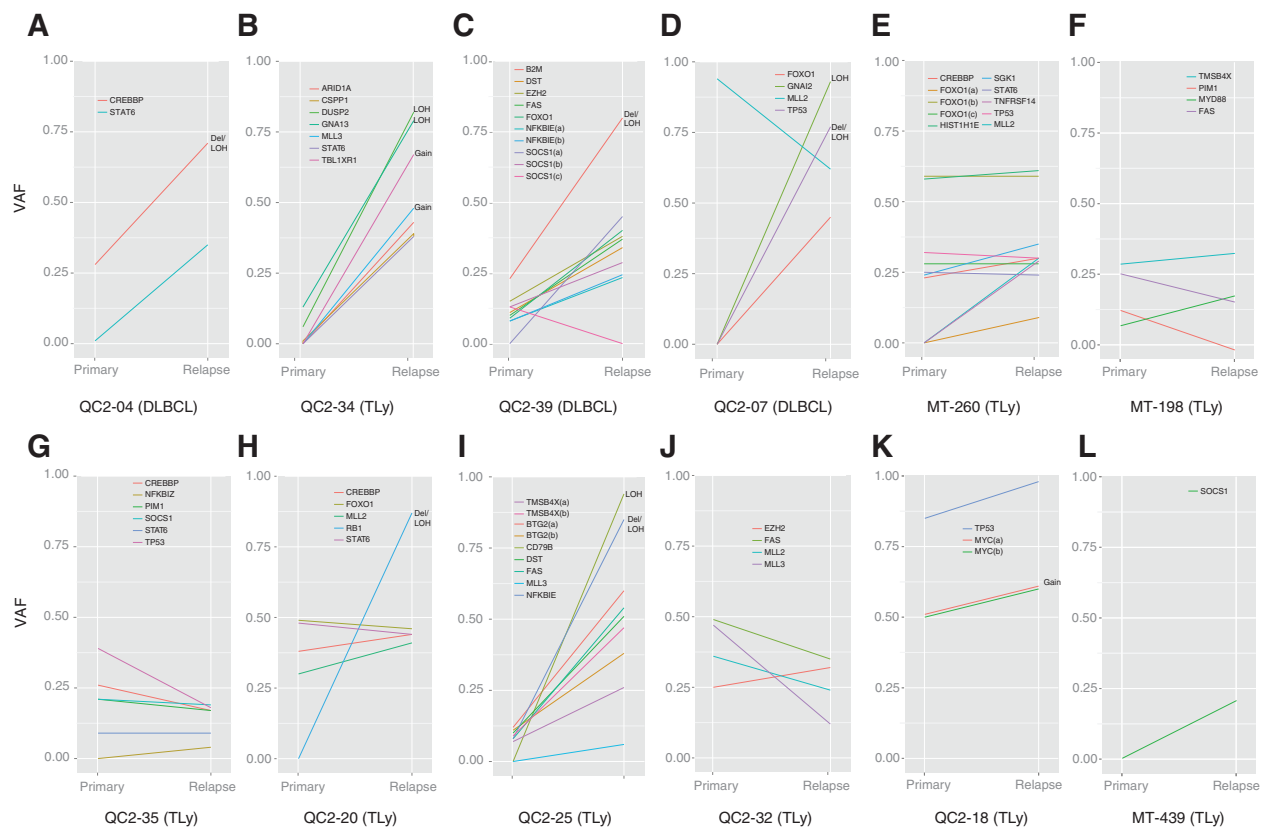


**Figure 2.**

Exploration of clonal expansions using matched diagnostic tumors. Deep amplicon sequencing of selected mutations in paired diagnostic and relapsed tumors across 12 patients (A–L) revealed multiple examples of clonal selection for known or suspected driver mutations including multiple examples of variants affecting JAK/STAT signaling. In QC2-34, there was no evidence for the mutant *STAT6* allele at diagnosis, whereas the VAF for other mutations likely to be clonal at diagnosis ranged from 6% to 13%, likely owing to low tumor content in this specimen. The *STAT6* mutation was therefore either subclonal at diagnosis and evaded detection, or was acquired in the intervening time prior to relapse. In QC2-04, it is evident that the reduced VAF in mutant *STAT6* in the diagnostic specimen (1%) was not due to tumor cellularity by observing a substantially higher VAF for a second mutation in the same sample (*CREBBP*; 28%). CNV can affect VAF, given that LOH was detected in *CREBBP* in the relapsed tumor, the increase in *CREBBP* VAF in that sample could be explained by this event. The large change in VAF for *STAT6*, however, can only be explained by this existing as a subclonal mutation at diagnosis. A third patient (QC2-39) harbored two mutations in the *STAT6*-regulator *SOCS1* in T2. One of these mutations was completely undetectable in the diagnostic tumor while a third mutation in this gene (absent at relapse) was found. Other examples of clonal expansions affected driver mutations associated with poor outcome in DLBCL or follicular lymphoma such as *FOXO1*, *TNFRSF14* and *TP53*. For example, QC2-07 showed acquisition of mutations in each of *TP53*, *GNAI2* and *FOXO1*. Although the *MLL2* mutation was preserved, none of these additional mutations were detectable in the diagnostic biopsy. In MT-260, mutations in both *HIST1H1E* and *TNFRSF14* were acquired and became clonal at relapse. A third acquired mutation, affecting *FOXO1*, was also acquired. Interestingly, this patient's tumor harbored two clonal *FOXO1* mutations at diagnosis. Counter-examples in which mutations affecting these genes were present at diagnosis but other driver mutations were acquired are also shown, including QC2-35 (*NFKB1Z*), QC2-20 (*RB1*) and QC2-25 (*CD79B* and *MLL3*). Also included are examples of patients in which evidence for clonal selection was unclear due to confounding issues of tumor purity (QC-32, QC2-18). For comparison, the VAFs that have been corrected for tumor content estimates and/or determined using a separate (capture-based) sequencing strategy are included in Supplementary Fig. S4 and Supplementary Table S6.

of 27 (15%) of *de novo* DLBCLs and 4 of 22 (18%) TLy, confirming these mutations are not restricted to TLy. We found evidence for intratumoral heterogeneity in a single TLy tumor that harbored two separate *STAT6* mutations. The VAF for one of these (E382K) was sufficiently high to indicate clonal representation (22.5%), whereas the VAF for the second mutation (D419G) was 2%, suggesting the presence of a subclone bearing this mutation. Interestingly, the pattern of *STAT6* mutations in untreated samples appeared different than that observed at relapse. Among the "relapse" tumors, 8 of 9 mutations affected D419, whereas in pretreatment samples, the mutation pattern was more heterogeneous, similar to that reported in PMBCL (Fig. 3A; ref. 21).

#### JAK/STAT signaling is a potential target in GCB rDLBCL and TLy

To address the impact of *STAT6* mutations in rDLBCL, we assessed the presence of activated nuclear phosphorylated *STAT6* protein (phospho-*STAT6*) using 25 of 27 rDLBCL FFPET samples. Phospho-*STAT6* was observed in 6 of 25 cases (24%), which was nuclear in 5 of 6 cases, and cytoplasmic in the other (Fig. 3B). Of the five nuclear cases, four had mutations in *STAT6* and one had three mutations in *SOCS1*, which encodes a negative regulator of *STAT6*. The case with cytoplasmic phospho-*STAT6* was wild type for both *STAT6* and *SOCS1*. Only one *STAT6* mutation was detected in the 18 phospho-*STAT6*-negative cases. Hence, the presence of *STAT6* mutations was significantly associated with the

Morin et al.

**Table 2.** Selected mutations showing clonal evolution between diagnostic (T1) and relapse (T2) tumors

Sample	Gene	Chr	Position	T1 VAF	T2 VAF	Method (T1)	Method (T2)	Effect	AA change
MT-260	<i>FOXO1</i>	13	41239736	0.00	0.09	Amplicon	Amplicon	Missense	S205N
MT-260	<i>MLL2</i>	12	49422605	0.00	0.26	Amplicon	Exome	Splice site	—
MT-260	<i>TNFRSF14</i>	1	2488166	0.00	0.29	Amplicon	Exome	Frameshift deletion	—
MT-198	<i>MYD88</i>	3	38182641	0.09	0.20	Capture	Capture	Missense	L273P
MT-439	<i>SOCS1</i>	16	11349134	0.00	0.22	Capture	Capture	Frameshift deletion	—
QC2-04	<i>STAT6</i>	12	57496661	0.01	0.35	Amplicon	Amplicon	Missense	D419G
QC2-07	<i>FOXO1</i>	13	41240280	0.01	0.45	Amplicon	Capture	Missense	T24A
QC2-07	<i>GNAI2</i>	3	50289546	0.00	0.93	Amplicon	Amplicon	Missense	G45W
QC2-07	<i>TP53</i>	17	7577563	0.00	0.77	Amplicon	Exome	Missense	S240G
QC2-20	<i>MLL2</i> <sup>a</sup>	12	49425950	0.30	0.41	Amplicon	Exome	Nonsense	Q4180 <sup>b</sup>
QC2-20	<i>CD79B</i>	17	62006660	0.00	0.36	Capture	Capture	Frameshift deletion	—
QC2-20	<i>CCND3</i>	6	41903688	0.00	0.35	Capture	Capture	Missense	I290R
QC2-20	<i>RB1</i>	13	48954198	0.01	0.77	Amplicon	Amplicon	Nonsense	R467 <sup>b</sup>
QC2-25	<i>CD79B</i>	17	62006799	0.00	0.94	Amplicon	Amplicon	Missense	Y197D
QC2-25	<i>NFKBIE</i>	6	44232738	0.08	0.85	Amplicon	Capture	Frameshift deletion	—
QC2-32	<i>EZH2</i> <sup>b</sup>	7	148508727	0.25	0.32	Amplicon	Amplicon	Missense	Y646S
QC2-34	<i>EZH2</i> <sup>b</sup>	7	148508728	0.14	0.25	Capture	Capture	Missense	Y646N
QC2-34	<i>BCL2</i> <sup>c</sup>	18	60985727	0.00	0.38	Capture	Capture	Missense	H58L
QC2-34	<i>MEF2B</i> <sup>c</sup>	19	19260045	0.00	0.47	Capture	Capture	Missense	D83V
QC2-34	<i>ARID1A</i>	1	27105930	0.00	0.43	Amplicon	Amplicon	Frameshift insertion	—
QC2-34	<i>MLL3</i>	7	152012367	0.00	0.48	Amplicon	Amplicon	Missense	D149V
QC2-34	<i>CSPPI</i>	8	67976692	0.00	0.39	Amplicon	Amplicon	Missense	E20G
QC2-34	<i>TBL1XR1</i>	3	176767901	0.00	0.67	Amplicon	Exome	Missense	W196R
QC2-34	<i>STAT6</i>	12	57496662	0.00	0.43	Amplicon	Amplicon	Missense	D419N
QC2-35	<i>TNFRSF14</i> <sup>b</sup>	1	2489818	0.16	0.11	Capture	Capture	Missense	G72D
QC2-35	<i>CARD11</i> <sup>b</sup>	7	2983887	0.11	0.11	Capture	Capture	Frameshift Deletion	—
QC2-35	<i>STAT6</i> <sup>b</sup>	12	57496662	0.17	0.12	Capture	Capture	Missense	D419H
QC2-35	<i>NFKBIZ</i>	3	101572431	0.00	0.04	Amplicon	Exome	Missense	A354D
QC2-39	<i>B2M</i>	15	45003746	0.23	0.80	Amplicon	Capture	Missense	M2R
QC2-39	<i>FOXO1</i>	13	41240015	0.09	0.40	Amplicon	Capture	Missense	G335A
QC2-39	<i>NFKBIE</i> <sup>b</sup>	6	44229483	0.08	0.23	Amplicon	Capture	Frameshift insertion	—
QC2-39	<i>SOCS1</i>	16	11349004	0.00	0.45	Amplicon	Capture	Missense	C332Y

NOTE: Suspected driver mutations identified in each tumor (T2) sample were selected for sequencing in T1 to assess their presence and clonal abundance at the time of diagnosis. Patients for which at least one mutation showed clear evidence for clonal evolution relative to other variants in the tumor are included. VAF changes likely resulting from variability in tumor cellularity between the samples are not shown.

Abbreviations: Chr, chromosome; T1, tumor at diagnosis; T2, tumor at relapse; VAF, variant allele fraction; AA, amino acid change where "—" predicts for a truncated protein.

<sup>a</sup>Adjustment of VAFs for tumor purity estimates affects whether these mutations underwent clonal expansion (see Supplementary Fig. S4). After adjustment, the VAF for the *EZH2* mutation in QC2-32 clearly increased at relapse, whereas the *NFKBIE* mutations in QC2-39 appear stable following correction for tumor purity.

<sup>b</sup>VAF change was not reproduced by a targeted capture-based sequencing of this sample (Supplementary Table S6).

<sup>c</sup>Additional mutations in this gene with similar VAF changes were detected in this sample and a representative is shown here.

presence of nuclear phospho-STAT6 protein ( $P = 0.021$ ), which is consistent with these mutations contributing to STAT6 activation.

To determine the transcriptional impact of mutations in this pathway, we compared the gene expression profile of patients with mutant and wild-type *STAT6*. We restricted the analysis to the GCB cases because *STAT6* mutations were present only in GCB and Tly cases. Given its known role in regulating this pathway and the presence of phospho-STAT6 in this case, we also included the single *SOCS1* mutant in the *STAT6*-mutant cohort. We first performed gene-set enrichment analysis on these groups using predefined gene sets for JAK/STAT signaling. JAK/STAT signaling was enriched in the *STAT6/SOCS1*-mutant samples compared with those lacking such mutations (NES =  $-1.31$ ; FDR =  $0.147$ ). The heatmap (Fig. 3C) demonstrates increased JAK/STAT signaling among the mutant DLBCLs, supporting previous reports that *STAT6* mutations activate *STAT6* and potentiate JAK/STAT signaling (22). Specifically, the mRNA expression of *FCER2*, *IL2RA*, and *SOCS1*, known *STAT6* target genes from the KEGG pathway were higher in mutants. Of the seven genes identified as specific mutant *STAT6* targets by Yildiz and colleagues, we had data on three, of which two were increased, but only *IL2RA* was statistically significant (22). In total, 10 of 24 (40%) of the cases that

were either Tly (5/13) or GCB-rDLBCL (5/11) had mutations in either *STAT6* or *SOCS1*, both of which were associated with active phospho-STAT6 protein and increased JAK/STAT6 signaling. Taken together, this pathway appears to be activated in rDLBCLs bearing mutations in *STAT6* or its regulators and therefore, may represent a new target for treatment in the relapse setting.

## Discussion

This study provides the genetic profile of the largest cohort of rDLBCL to date and to our knowledge, the first time that exome sequencing was performed in rDLBCL samples obtained within the context of a clinical trial. We show that known lymphoma-related genes, as well as some novel genes not previously associated with *de novo* DLBCL, were frequently mutated at the time of relapse and, in some cases, significantly more than in untreated DLBCL patients. In addition to being more commonly mutated in this cohort, each of *TP53*, *MLL3*, *NFKBIZ*, *STAT6*, *FOXO1*, and *CCND3* were also found to have undergone clonal enrichment between diagnosis and relapse. Our combined exome and targeted sequencing approach also identified novel and subclonal mutations that may have otherwise gone undetected if sequencing

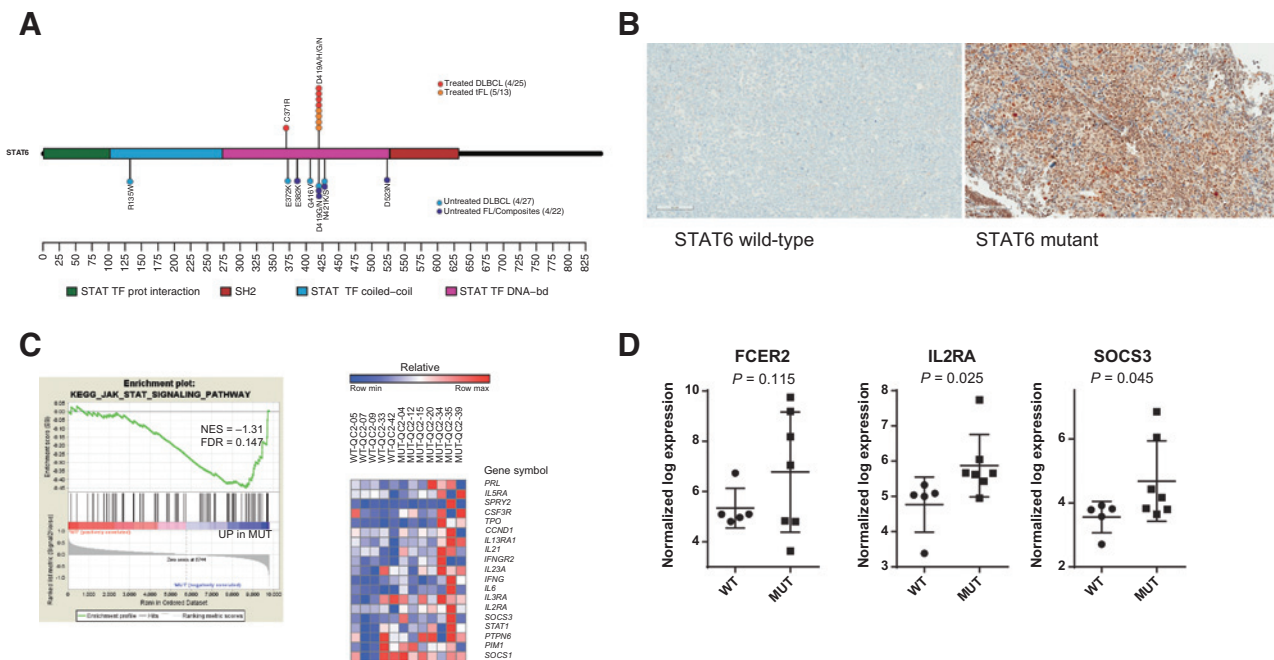


**Figure 3.**

Activation of the JAK/STAT pathway in *STAT6* and *SOCS1*-mutant lymphoma cells. A, in all but one of the *STAT6*-mutated rrDLBCL cases interrogated either by exome or targeted sequencing ( $n = 7/8$ ), the mutation affected at a single amino acid (D419) in the DNA-binding domain (DBD). In these samples, this residue was replaced by any of histidine (1), alanine (1), glycine (2), and asparagine (2). Although mutations in this residue have been observed in PMBCL, the other mutations in the DBD appear to be more common in that malignancy (17). Sequencing of *STAT6* in the extended set of 27 untreated DLBCLs and 22 Tly revealed a less focal pattern of mutations. B, representative images of nuclear phospho-STAT6 protein expression of *STAT6* wild type rrDLBCL and *STAT6* mutant rrDLBCL. C, gene-set enrichment analysis comparing *STAT6* wild-type and *STAT6* mutant GCB-type rrDLBCL show that the KEGG-annotated JAK/STAT pathway is enriched in *STAT6* mutants. The heatmap shows genes in the KEGG JAK/STAT pathway that are enriched in the mutant samples. D, mutant *STAT6* target mRNAs (*FCER2*, *IL2RA*, and *SOCS3*) are increased in lymphomas harboring mutations in *STAT6* or *SOCS1*.

candidate genes based on prior knowledge of DLBCL, for example, recurrent indels in *NFKBIE* and missense mutations in *NFKBIZ*. We note that reliance solely on exome sequencing can yield insufficient sequence coverage for some genes, as illustrated by the low yield of *FOXO1* mutations across the exomes, thereby demonstrating value for using a combination of global and targeted techniques if sequencing were used to evaluate biomarkers of response in clinical trials.

Our data may inform on the design and interpretation of clinical trials studying the activity of targeted therapies. The frequencies of *MYD88* and *CD79B* mutations in our ABC rrDLBCLs were similar to those obtained by Wilson and colleagues, supporting that our genomic data is representative of other rrDLBCL patients undergoing clinical trials (39). One important finding in our study is that deep sequencing of diagnostic biopsies can miss mutations that become clonally enriched at relapse, providing a rationale for obtaining another biopsy at the time of progression, especially in patients enrolling in clinical trials. Specifically, we show that many mutations involved in regulating NF- $\kappa$ B signaling can become clonally enriched at relapse (Table 2). The most commonly mutated genes involved were *CD79B* and *MYD88*, a pattern that is similar to *de novo* DLBCL. In addition, two regulators of NF- $\kappa$ B signaling, *NFKBIE* and *NFKBIZ*, which were under-represented in *de novo* DLBCL, may play a role in approximately 18% of rrDLBCL. Thus, testing for these mutations in patients treated with NF- $\kappa$ B-targeted therapies, especially in clinical trials, may be indicated. Another important observation is

that we provide insights into the biology of GCB-rrDLBCL, a COO subtype in need of novel therapies and that represents half of the patients with rrDLBCL entering clinical trials (40–42). This is counterintuitive because one might expect patients with the ABC subtype to be over-represented at the time of relapse, given their poor prognosis with RCHOP. We also demonstrate that the mutation spectrum of rrGCB-DLBCL and rrTly are very similar after therapy and generally distinguishable from ABC-rrDLBCL, providing a rationale for including patients with rrTly on more rrDLBCL clinical trials, especially those investigating emerging therapeutics that specifically target GCB-associated pathways, for example, inhibitors of *EZH2* activity (43).

This study prioritizes genes for future research focused on understanding therapeutic resistance in DLBCL. Our work directly complements previous studies of rrDLBCL that were underpowered to detect mutations that were significantly more common at relapse (19, 20). *TP53* emerged as a top candidate in our analyses, an expected result that supports our analytic approach. *TP53* mutations are associated with RCHOP resistance and are selected for by DNA-damaging agents (44, 45). The novelty here is that we demonstrate examples of mutant VAF for *TP53* exceeding 50% in rrDLBCL, suggesting a tendency towards loss of the wild-type allele under the selective pressure of immunochemotherapy. This has important therapeutic implications, demonstrating the necessity of treatments for rrDLBCL that act independently of *TP53*. The increased frequency of *FOXO1* mutations was also not surprising given their negative prognostic role in *de novo* DLBCL, but the

trend towards acquisition of such mutations by clonal expansions following treatment has not been reported (29). We have also identified genes known to play a role in other lymphoid malignancies as having a probable role in DLBCL relapse, namely *STAT6*, *FAS*, *CCND3*, and *NFKBIE*. In contrast, the notably lower frequency of mutations in *TMEM30A*, *EP300*, *SGK1*, *CD58*, *MEF2B*, *B2M*, and *PRDM1* in rDLBCL relative to untreated cohorts, though not statistically significant, might suggest they are not associated with RCHOP resistance or may represent a more curable group of tumors.

The presence of *STAT6* mutations in approximately 40% of patients with GCB-type rDLBCL and Tly promote JAK/STAT signaling as a novel therapeutic target for these patients. *STAT6* mutations, including D419, have been mostly reported in PMBCL and follicular lymphoma (18, 21). Wild-type phospho-*STAT6* protein is not expressed in *de novo* DLBCL, but is expressed in most cases of PMBCL and HL, two lymphoma subtypes that are associated with very high cure rates (21, 46). Thus, it is unlikely that wild-type *STAT6* induces chemoresistance, but rather the mutated version of *STAT6*, specifically at residue D419 in the DNA-binding domain, which appears to be selected for after chemotherapy in rDLBCL. The oncogenic function of mutated *STAT6* D419 has not been elucidated, but the increased nuclear localization of phospho-*STAT6* D419, increased expression of some *STAT6* target genes, and the selection for a mutation that changes an amino acid at a single site, D419, are all consistent with its role as an activating mutation that promotes the survival of rDLBCL and Tly (22). Supporting this, *STAT6*-D419-mutated PMBCL cell lines depend on *STAT6* signaling for their survival and are more sensitive to JAK2 inhibitors compared with *STAT6* wild-type PMBCL cell lines (23, 47). Other mechanisms of increased JAK/STAT signaling have been reported in diagnostic DLBCL samples, such as mutations in *SOCS1* and *STAT3* (48, 49). However, these occurred in less than 5% of our cohort, suggesting that JAK/STAT signaling at relapse is predominantly driven by *STAT6* mutations and represents a new therapeutic target for patients with Tly and r-GCB-DLBCL (48, 49). Given that JAK2 inhibitors are routinely used to treat JAK2-mutated myeloproliferative disorders, and they are active in *STAT6*-mutant PMBCL cell lines, they could be readily tested in the setting of *STAT6*-mutated rDLBCL in future clinical trials.

We provide a comprehensive genome analysis of rDLBCL samples acquired after therapy that is representative of the patient population enrolling in clinical trials and in whom novel targeted therapies would be considered. Our data confirm the work by Jiang and colleagues who showed that clonal evolution occurs in DLBCL under the selection pressure of RCHOP and subsequent therapies, by showing clonal enrichment of one or more mutation in 11 of 12 paired samples (19). A repeat biopsy at the time of relapse would therefore be warranted if the tumor biology were guiding the choice of therapy. Although our data support clonal selection for mutations in more than 20 genes across these cases, *TP53*, *STAT6*, *MLL3*, *CCND3*, and *FOXO1* each have the greatest support for having a role in therapeutic resistance owing to significantly greater prevalence in our cohort. Future work on larger cohorts and paired specimens is needed to further prioritize individual mutations in these genes that are clinically significant. Identifying genes that are not known to play a role in *de novo* DLBCL, but are recurrently mutated in rDLBCL, is also novel. These included *FAS*, *STAT6*, *NFKBIZ*, and *NFKBIE*. Our work has

highlighted that *STAT6* mutations correlate with the presence of phospho-*STAT6* protein. This may be a biomarker of activated JAK/STAT signaling and a potential novel therapeutic opportunity for patients with GCB-rDLBCL and Tly, patients in whom targeted therapies are needed. Finally, we have shown that the combination of exome and targeted sequencing within the context of a clinical trial is feasible. This can be useful to identify biomarkers of response to tested therapies and importantly, provide a valuable opportunity to gain further insights into the mechanisms of RCHOP resistance in DLBCL.

### Disclosure of Potential Conflicts of Interest

S.E. Assouline reports receiving commercial research grants from Novartis, speakers bureau honoraria from Janssen, and is a consultant/advisory board member for Lundbeck. N.A. Johnson reports receiving commercial research grants from Roche, speakers bureau honoraria from Roche Canada, and Seattle Genetics, and is a consultant/advisory board member for Abbvie, Gilead, Janssen, Lundbeck, and Roche. No potential conflicts of interest were disclosed by the other authors.

### Authors' Contributions

**Conception and design:** R.D. Morin, S. Assouline, T. Petrogiannis-Halioitis, K.K. Mann, N.A. Johnson

**Development of methodology:** R.D. Morin, S. Assouline, M. Alcaide, Y. Riazalhosseini, K.K. Mann, N.A. Johnson

**Acquisition of data (provided samples, acquired and managed patients, provided facilities, etc.):** R.D. Morin, S. Assouline, R.L. Johnston, S. Yu, T.H. Nielsen, M. Crump, A. Tosikyan, D. MacDonald, C. Rousseau, M. Bayat, Y. Monczak, Y. Riazalhosseini, E. Camlioglu, A.M. Constantin, Q. Pan-Hammarstrom, R. Peng, K.K. Mann, N.A. Johnson

**Analysis and interpretation of data (e.g., statistical analysis, biostatistics, computational analysis):** R.D. Morin, S. Assouline, T. Petrogiannis-Halioitis, M. Alcaide, A. Mohajeri, R.L. Johnston, L. Chong, J. Grewal, D. Fornika, B.M. Grande, P. Sesques, M. Albuquerque, K.K. Oros, C. Greenwood, M. Arseneault, K.K. Mann, N.A. Johnson

**Writing, review, and/or revision of the manuscript:** R.D. Morin, S. Assouline, J. Grewal, D. Fornika, T.H. Nielsen, T. Petrogiannis-Halioitis, M. Crump, A. Tosikyan, D. MacDonald, C. Rousseau, P. Sesques, Y. Monczak, K.K. Oros, C. Greenwood, M. Arseneault, A.M. Constantin, K.K. Mann, N.A. Johnson

**Administrative, technical, or material support (i.e., reporting or organizing data, constructing databases):** S. Assouline, A. Mohajeri, R.L. Johnston, L. Chong, D. Fornika, K. Bushell, T. Petrogiannis-Halioitis, B.M. Grande, C. Rousseau, R. Froment, M. Arseneault

**Study supervision:** R.D. Morin, S. Assouline, M. Arseneault, K.K. Mann, N.A. Johnson

**Other (experimental work):** A. Mohajeri

### Grant Support

This work received funding from Roche Canada and Novartis. It was also supported by the Canadian Institute for Health Research (CIHR; operating grants 300738, awarded to R.D. Morin and N.A. Johnson; 299607, awarded to N.A. Johnson), the Canadian Cancer Society Research Institute innovation grant (703425; awarded to N.A. Johnson), the Terry Fox Research Institute (#1043; awarded to R.D. Morin), Genome Canada and Genome British Columbia, the BC Cancer Foundation and the Jewish General Hospital Foundation. R.D. Morin is supported by a CIHR New Investigator award and N.A. Johnson and S.E. Assouline receive salary support from Fond de Recherche en Sante du Quebec. Q. Pan-Hammarstrom is supported by the Swedish Cancer Society and the Swedish Children Cancer Fund.

The costs of publication of this article were defrayed in part by the payment of page charges. This article must therefore be hereby marked *advertisement* in accordance with 18 U.S.C. Section 1734 solely to indicate this fact.

Received August 30, 2015; revised October 26, 2015; accepted November 17, 2015; published OnlineFirst December 8, 2015.

## References

- Coiffier B, Lepage E, Briere J, Herbrecht R, Tilly H, Bouabdallah R, et al. CHOP chemotherapy plus rituximab compared with CHOP alone in elderly patients with diffuse large-B-cell lymphoma. *N Engl J Med* 2002;346:235–42.
- Alizadeh AA, Eisen MB, Davis RE, Ma C, Lossos IS, Rosenwald A, et al. Distinct types of diffuse large B-cell lymphoma identified by gene expression profiling. *Nature* 2000;403:503–11.
- Lenz G, Wright G, Dave SS, Xiao W, Powell J, Zhao H, et al. Stromal gene signatures in large-B-cell lymphomas. *N Engl J Med* 2008;359:2313–23.
- Kuruvilla J, MacDonald DA, Kouroukis CT, Cheung M, Olney HJ, Turner AR, et al. Salvage chemotherapy and autologous stem cell transplantation for transformed indolent lymphoma: a subset analysis of NCIC CTG LY12. *Blood* 2015;126:733–8.
- Morin RD, Mendez-Lago M, Mungall AJ, Goya R, Mungall KL, Corbett RD, et al. Frequent mutation of histone-modifying genes in non-Hodgkin lymphoma. *Nature* 2011;476:298–303.
- Morin RD, Johnson NA, Severson TM, Mungall AJ, An J, Goya R, et al. Somatic mutations altering EZH2 (Tyr641) in follicular and diffuse large B-cell lymphomas of germinal-center origin. *Nat Genet* 2010;42:181–5.
- Morin RD, Mungall K, Pleasance E, Mungall AJ, Goya R, Huff RD, et al. Mutational and structural analysis of diffuse large B-cell lymphoma using whole-genome sequencing. *Blood* 2013;122:1256–65.
- Pasqualucci L, Trifonov V, Fabbri G, Ma J, Rossi D, Chiarenza A, et al. Analysis of the coding genome of diffuse large B-cell lymphoma. *Nat Genet* 2011;43:830–7.
- Zhang J, Grubor V, Love CL, Banerjee A, Richards KL, Mieczkowski PA, et al. Genetic heterogeneity of diffuse large B-cell lymphoma. *Proc Natl Acad Sci U S A* 2013;110:1398–403.
- Lohr JG, Stojanov P, Lawrence MS, Auclair D, Chapuy B, Sougnez C, et al. Discovery and prioritization of somatic mutations in diffuse large B-cell lymphoma (DLBCL) by whole-exome sequencing. *Proc Natl Acad Sci U S A* 2012;109:3879–84.
- Challa-Malladi M, Lieu YK, Califano O, Holmes AB, Bhagat G, Murty VV, et al. Combined genetic inactivation of beta2-Microglobulin and CD58 reveals frequent escape from immune recognition in diffuse large B cell lymphoma. *Cancer Cell* 2011;20:728–40.
- Pasqualucci L, Dominguez-Sola D, Chiarenza A, Fabbri G, Grunn A, Trifonov V, et al. Inactivating mutations of acetyltransferase genes in B-cell lymphoma. *Nature* 2011;471:189–95.
- Davis RE, Ngo VN, Lenz G, Tolar P, Young RM, Romesser PB, et al. Chronic active B-cell-receptor signalling in diffuse large B-cell lymphoma. *Nature* 2010;463:88–92.
- Lenz G, Davis RE, Ngo VN, Lam L, George TC, Wright GW, et al. Oncogenic CARD11 mutations in human diffuse large B cell lymphoma. *Science* 2008;319:1676–9.
- Ngo VN, Young RM, Schmitz R, Jhavar S, Xiao W, Lim KH, et al. Oncogenically active MYD88 mutations in human lymphoma. *Nature* 2011;470:115–9.
- Compagno M, Lim WK, Grunn A, Nandula SV, Brahmachary N, Shen Q, et al. Mutations of multiple genes cause deregulation of NF-kappaB in diffuse large B-cell lymphoma. *Nature* 2009;459:717–21.
- Pasqualucci L, Khiabanian H, Fangazio M, Vasishtha M, Messina M, Holmes AB, et al. Genetics of follicular lymphoma transformation. *Cell Rep* 2014;6:130–40.
- Okosun J, Bodor C, Wang J, Araf S, Yang CY, Pan C, et al. Integrated genomic analysis identifies recurrent mutations and evolution patterns driving the initiation and progression of follicular lymphoma. *Nat Genet* 2014;46:176–81.
- Jiang Y, Redmond D, Nie K, Eng KW, Clozel T, Martin P, et al. Deep sequencing reveals clonal evolution patterns and mutation events associated with relapse in B-cell lymphomas. *Genome Biol* 2014;15:432.
- de Miranda NF, Georgiou K, Chen L, Wu C, Gao Z, Zaravinos A, et al. Exome sequencing reveals novel mutation targets in diffuse large B-cell lymphomas derived from Chinese patients. *Blood* 2014;124:2544–53.
- Ritz O, Gütter C, Castellano F, Dorsch K, Melzner J, Jais JP, et al. Recurrent mutations of the STAT6 DNA binding domain in primary mediastinal B-cell lymphoma. *Blood* 2009;114:1236–42.
- Yildiz M, Li H, Bernard D, Amin NA, Ouillette P, Jones S, et al. Activating STAT6 mutations in follicular lymphoma. *Blood* 2015;125:668–79.
- Ritz O, Rommel K, Dorsch K, Kelsch E, Melzner J, Buck M, et al. STAT6-mediated BCL6 repression in primary mediastinal B-cell lymphoma (PMBL). *Oncotarget* 2013;4:1093–102.
- Swerdlow SH, Campo E, Harris NL, Jaffe ES, Pileri S, Stein H, et al. WHO Classification of tumours of haematopoietic and lymphoid tissues: IARC: Lyon, France; 2008.
- Nielsen TH, Diaz Z, Christodoulopoulos R, Charbonneau F, Qureshi S, Rousseau C, et al. Methods for sample acquisition and processing of serial blood and tumor biopsies for multicenter diffuse large B-cell lymphoma clinical trials. *Cancer Epidemiol Biomarkers Prev* 2014;23:2688–93.
- Hans CP, Weisenburger DD, Greiner TC, Gascoyne RD, Delabie J, Ott G, et al. Confirmation of the molecular classification of diffuse large B-cell lymphoma by immunohistochemistry using a tissue microarray. *Blood* 2004;103:275–82.
- Saunders CT, Wong WS, Swamy S, Becq J, Murray LJ, Cheetham RK, Strelka: accurate somatic small-variant calling from sequenced tumor-normal sample pairs. *Bioinformatics* 2012;28:1811–7.
- Ha G, Roth A, Khattraj J, Ho J, Yap D, Prentice LM, et al. TITAN: inference of copy number architectures in clonal cell populations from tumor whole-genome sequence data. *Genome Res* 2014;24:1881–93.
- Trinh DL, Scott DW, Morin RD, Mendez-Lago M, An J, Jones SJ, et al. Analysis of FOXO1 mutations in diffuse large B-cell lymphoma. *Blood* 2013;121:3666–74.
- Wright G, Tan B, Rosenwald A, Hurt EH, Wiestner A, Staudt LM. A gene expression-based method to diagnose clinically distinct subgroups of diffuse large B cell lymphoma. *Proc Natl Acad Sci U S A* 2003;100:9991–6.
- Schmitz R, Young RM, Ceribelli M, Jhavar S, Xiao W, Zhang M, et al. Burkitt lymphoma pathogenesis and therapeutic targets from structural and functional genomics. *Nature* 2012;490:116–20.
- Bahram F, von der Lehr N, Cetinkaya C, Larsson LG. c-Myc hot spot mutations in lymphomas result in inefficient ubiquitination and decreased proteasome-mediated turnover. *Blood* 2000;95:2104–10.
- Li Z, Nabel GJ. A new member of the I kappaB protein family, I kappaB epsilon, inhibits RelA (p65)-mediated NF-kappaB transcription. *Mol Cell Biol* 1997;17:6184–90.
- Alves BN, Tsui R, Almaden J, Shokhirev MN, Davis-Turak J, Fujimoto J, et al. IkappaBepsilon is a key regulator of B cell expansion by providing negative feedback on cRel and RelA in a stimulus-specific manner. *J Immunol* 2014;192:3121–32.
- Emmerich F, Theurich S, Hummel M, Haeffker A, Vry MS, Dohner K, et al. Inactivating I kappa B epsilon mutations in Hodgkin/Reed-Sternberg cells. *J Pathol* 2003;201:413–20.
- Domenech E, Gomez-Lopez G, Gzlez-Pena D, Lopez M, Herreros B, Menezes J, et al. New mutations in chronic lymphocytic leukemia identified by target enrichment and deep sequencing. *PLoS One* 2012;7:e38158.
- Mansouri L, Sutton LA, Ljungstrom V, Bondza S, Arngarden L, Bhoi S, et al. Functional loss of IkappaBepsilon leads to NF-kappaB deregulation in aggressive chronic lymphocytic leukemia. *J Exp Med* 2015;212:833–43.
- Nogai H, Wenzel SS, Hailfinger S, Grau M, Kaergel E, Seitz V, et al. IkappaB-zeta controls the constitutive NF-kappaB target gene network and survival of ABC DLBCL. *Blood* 2013;122:2242–50.
- Wilson WH, Young RM, Schmitz R, Yang Y, Pittaluga S, Wright G, et al. Targeting B cell receptor signaling with ibrutinib in diffuse large B cell lymphoma. *Nat Med* 2015;21:922–6.
- Dunleavy K, Pittaluga S, Czuczman MS, Dave SS, Wright G, Grant N, et al. Differential efficacy of bortezomib plus chemotherapy within molecular subtypes of diffuse large B-cell lymphoma. *Blood* 2009;113:6069–76.
- Hernandez-Ilizaliturri FJ, Deeb G, Zinzani PL, Pileri SA, Malik F, Macon WR, et al. Higher response to lenalidomide in relapsed/refractory diffuse large B-cell lymphoma in nongermlinal center B-cell-like than in germinal center B-cell-like phenotype. *Cancer* 2011;117:5058–66.
- Thieblemont C, Briere J, Mounier N, Voelker HU, Cucchini W, Hirschaud E, et al. The germinal center/activated B-cell subclassification has a prognostic impact for response to salvage therapy in relapsed/refractory diffuse large B-cell lymphoma: a bio-CORAL study. *J Clin Oncol* 2011;29:4079–87.
- McCabe MT, Ott HM, Ganji G, Korenchuk S, Thompson C, Van Aller GS, et al. EZH2 inhibition as a therapeutic strategy for lymphoma with EZH2-activating mutations. *Nature* 2012;492:108–12.

Morin et al.

44. Xu-Monette ZY, Wu L, Visco C, Tai YC, Tzankov A, Liu WM, et al. Mutational profile and prognostic significance of TP53 in diffuse large B-cell lymphoma patients treated with R-CHOP: report from an International DLBCL Rituximab-CHOP Consortium Program Study. *Blood* 2012;120:3986–96.
45. Malina A, Mills JR, Cencic R, Yan Y, Fraser J, Schippers LM, et al. Repurposing CRISPR/Cas9 for in situ functional assays. *Genes Dev* 2013;27:2602–14.
46. Skinnider BF, Elia AJ, Gascoyne RD, Patterson B, Trumper L, Kapp U, et al. Signal transducer and activator of transcription 6 is frequently activated in Hodgkin and Reed-Sternberg cells of Hodgkin lymphoma. *Blood*. 2002;99:618–26.
47. Ritz O, Guiter C, Dorsch K, Dusanter-Fourt I, Wegener S, Jouault H, et al. STAT6 activity is regulated by SOCS-1 and modulates BCL-XL expression in primary mediastinal B-cell lymphoma. *Leukemia* 2008;22:2106–10.
48. Ok CY, Chen J, Xu-Monette ZY, Tzankov A, Manyam GC, Li L, et al. Clinical implications of phosphorylated STAT3 expression in De Novo diffuse large B-cell lymphoma. *Clin Cancer Res* 2014;20:5113–23.
49. Schif B, Lennerz JK, Kohler CW, Bentink S, Kreuz M, Melzner I, et al. SOCS1 mutation subtypes predict divergent outcomes in diffuse large B-cell lymphoma (DLBCL) patients. *Oncotarget* 2013;4:35–47.

# Clinical Cancer Research

## Genetic Landscapes of Relapsed and Refractory Diffuse Large B-Cell Lymphomas

Ryan D. Morin, Sarit Assouline, Miguel Alcaide, et al.

*Clin Cancer Res* 2016;22:2290-2300. Published OnlineFirst December 8, 2015.

**Updated version** Access the most recent version of this article at:  
[doi:10.1158/1078-0432.CCR-15-2123](https://doi.org/10.1158/1078-0432.CCR-15-2123)

**Supplementary Material** Access the most recent supplemental material at:  
<http://clincancerres.aacrjournals.org/content/suppl/2015/12/07/1078-0432.CCR-15-2123.DC1>

**Cited articles** This article cites 48 articles, 24 of which you can access for free at:  
<http://clincancerres.aacrjournals.org/content/22/9/2290.full#ref-list-1>

**Citing articles** This article has been cited by 16 HighWire-hosted articles. Access the articles at:  
<http://clincancerres.aacrjournals.org/content/22/9/2290.full#related-urls>

**E-mail alerts** [Sign up to receive free email-alerts](#) related to this article or journal.

**Reprints and Subscriptions** To order reprints of this article or to subscribe to the journal, contact the AACR Publications Department at [pubs@aacr.org](mailto:pubs@aacr.org).

**Permissions** To request permission to re-use all or part of this article, use this link  
<http://clincancerres.aacrjournals.org/content/22/9/2290>.  
Click on "Request Permissions" which will take you to the Copyright Clearance Center's (CCC) Rightslink site.